DNA Polymerase β Fidelity: Halomethylene-Modified Leaving Groups in Pre-Steady-State Kinetic Analysis Reveal Differences at the Chemical Transition State†

Christopher A. Sucato,‡ Thomas G. Upton,‡ Boris A. Kashemirov,‡ Jorge Osuna,‡ Keriann Oertell,‡ William A. Beard,§ Samuel H. Wilson,§ Jan Florián,⊥ Arieh Warshel,‡ Charles E. McKenna,‡ and Myron F. Goodman*,‡,△

Departments of Biological Sciences and Chemistry, University of Southern California, Los Angeles, California 90089, Department of Chemistry, Loyola University Chicago, Chicago, Illinois 60626, and Laboratory of Structural Biology, NIEHS, National Institutes of Health, Research Triangle Park, North Carolina 27709

Received July 18, 2007; Revised Manuscript Received November 8, 2007

ABSTRACT: The mechanism of DNA polymerase β-catalyzed nucleotidyl transfer consists of chemical steps involving primer 3′ OH deprotonation, nucleophilic attack, and pyrophosphate leaving-group elimination, preceded by dNTP binding which induces a large-amplitude conformational change for Watson−Crick nascent base pairs. Ambiguity in the nature of the rate-limiting step and active-site structural differences between correct and incorrect base-paired transition states remain obstacles to understanding DNA replication fidelity. Analogues of dGTP where the β-γ bridging oxygen is replaced with fluorine-substituted methylene groups have been shown to probe the contribution of leaving-group elimination to the overall catalytic rate (*Biochemistry 46,* 461−471). Here, the analysis is expanded substantially to include a broad range of halogen substituents with disparate steric and electronic properties. Evaluation of linear free energy relationships for incorporation of dGTP analogues opposite either template base C or T reveals a strong correlation of log(k_{pol}) to leaving group pK_a. Significantly different k_{pol} behavior is observed with a subset of the analogues, with magnitude dependent on the identity of the nascent base pair. This observation, and the absence of an analogous effect on ground state analogue binding (K_d values), points to active-site structural differences at the chemical transition state. Reduced catalysis with bulky halo-containing substrates is manifested in the fidelity of T-G incorporation, where the CCl_2-bridging analogue shows a 27-fold increase in fidelity over the natural dGTP. Solvent pH and deuterium isotope-effect data are also used to evaluate mechanistic differences between correct and mispaired incorporation.

The molecular-level characterization of DNA polymerase β (pol[1] β)-catalyzed nucleotidyl transfer is an active area of structural (*1*−*4*), kinetic (*5*−*8*), and computational (*9*−*12*) research, as pol β is considered a model system for understanding the nature of polymerase substrate specificity (*13*) and thus a key component of maintaining genomic integrity. Interest in pol β is underscored because of its role in removing damaged nucleotides and abasic sites via the base excision repair pathway, a series of enzymatic steps critical in repairing damage to DNA from endogenous or exogenous reactive oxygen species and alkylating agents (*14*). Mutant forms of pol β are found in a high percentage of human carcinomas (*15, 16*), suggesting a link between pol β activity and carcinogenesis which is yet to be fully understood.

Pol β has a 31 kDa polymerase domain with three subdomains having separate roles in binding and orienting Mg^{2+} cofactors, dsDNA, and the nascent base pair. X-ray crystallography on pol β in various liganded states (*1, 3, 17*−*19*) has identified large-amplitude movements of the subdomains when the nascent base pair conforms to Watson−Crick geometry, forming a closed ternary pol−DNA−dNTP complex. Mismatched nascent base pairs leading to single base substitution errors have proven more difficult to characterize in ternary complexes but are believed to be incorporated from a structurally distinct conformation (*20*−*24*). A comprehensive review of the structural and mechanistic studies on pol β, spanning some 35 years, has recently appeared (*20*). Consensus from numerous spectroscopic studies of conformational dynamics (*6, 7, 25*−*27*) is that the large-amplitude conformational change associated with initial dNTP binding is too fast to be rate-limiting in the pol β mechanism. Thus, attention has focused on more subtle side-chain rearrangements near the active site, and the

† This work was supported in part by the Intramural Research Program of the NIH, National Institute of Environmental Health Sciences, and by National Institutes of Health grants 1U19CA10501 and R37GM21422. J.O. is a PREP Scholar at USC.

* To whom correspondence should be addressed. Telephone: (213) 740-5190. Fax: (213) 740-8631. E-mail: mgoodman@usc.edu.

‡ Department of Chemistry, University of Southern California.

⊥ Loyola University.

§ NIEHS.

△ Department of Biological Sciences, University of Southern California.

[1] Abbreviations: pol, DNA polymerase; dsDNA, double-stranded DNA; LFER, linear free energy relationship; nt, nucleotide; $O_{\alpha\beta}$, α-β bridging triphosphate oxygen; $O_{\beta\gamma}$, β-γ bridging triphosphate oxygen; P_α, dNTP α phosphorus; EVB, empirical valence bond; FEP, free energy perturbation; KIE, kinetic isotope effect; RdRp, RNA-dependent RNA polymerase.

10.1021/bi7014162 CCC: $40.75
Published on Web 12/28/2007

chemical steps in the reaction pathway (primer 3′ hydroxyl deprotonation nucleophilic attack on the dNTP α phosphorus, and pyrophosphate leaving-group elimination).

Until recently, the only direct probe of chemical steps was thio-substitution for a nonbridging oxygen on P_α of the dNTP (*20*, *28*, *29*). Thio-substitution should destabilize nucleophilic attack on P_α and therefore raise the activation barrier of chemistry relative to nonbridging oxygen (*30*, *31*), allowing for a test of whether or not chemical activation barriers dominate the reaction pathway. As has been described in detail (*20*, *28*, *29*), however, interpretation of thio-effect data is complicated by pol β stereoselectivity for the *S*p isomer of dATPαS and steric considerations that lead to uncertainty in assigning a proper reference thio-effect (*32*) with which to compare that measured in the enzyme. In a recent article, we introduced the use of dNTP analogues modified at the β-γ bridging oxygen as a probe of the chemical step of leaving group elimination ($P_\alpha-O_{\alpha\beta}$ bond breaking) in pol β for both correct and mispair incorporation (*5*). Analyzing the transient kinetics of a series of such compounds according to a linear free energy relationship (LFER) offers key advantages over dNTPαS substrates.

Unlike thio-substitution which is limited to comparing the differential activity of oxygen versus sulfur substituents, β-γ modification has been shown to accommodate a range of halomethylene groups having diverse steric and electronic properties (*5*). The β-γ bridging position is observed to protrude into a solvent exposed cleft so that, within some bounds, the leaving-group ability and steric profile can be varied to gain a high degree of "leverage" on the $P_\alpha-O_{\alpha\beta}$ bond-breaking activation barrier without grossly perturbing active site geometry (Figure 1A). Additionally, the β-γ bridging position is not in the coordination sphere of Mg^{2+} cofactors, unlike one of the nonbridging oxygens of P_α which stereospecifically interacts with both metal cations (*3*, *17*).

In the previous work with a limited number of analogues, we observed Brønsted plots (log k_{pol} versus leaving group pK_a) with a linear region of steep slope adjacent to a region of reduced catalytic sensitivity at stronger stabilization of leaving group elimination (*5*), leading to a proposed LFER model where two or more activation barriers lie close in height. Trends for both correct and mispair incorporation appeared similar. Here, we expand the analysis to include a much broader range of halomethylene replacements for $O_{\beta\gamma}$ (Figure 1B), which significantly increases the number of interpolating points and the steric/electronic properties at the β-γ bridging position. We find additional evidence supporting the existence of regions of steep slope and thus a rate-limiting chemical step. Importantly, however, the different behavior of a subset of the analogues comparing correct and mispair incorporation points to structural differences in the active site of these two processes, possibly in the conformation of the triphosphate moiety in coordination with Mg^{2+} and/or the position of Arg183 relative to $O_{\beta\gamma}$. Proton transfers, which remain a relatively unexplored avenue in the pol β reaction pathway, were also investigated by varying the pH and solvent deuterium isotope content. Differences in the D_2O-effect on k_{pol} and K_d, dependent on the nascent base pair, support the LFER data suggesting mechanistic disparities between correct and mispair incorporation.

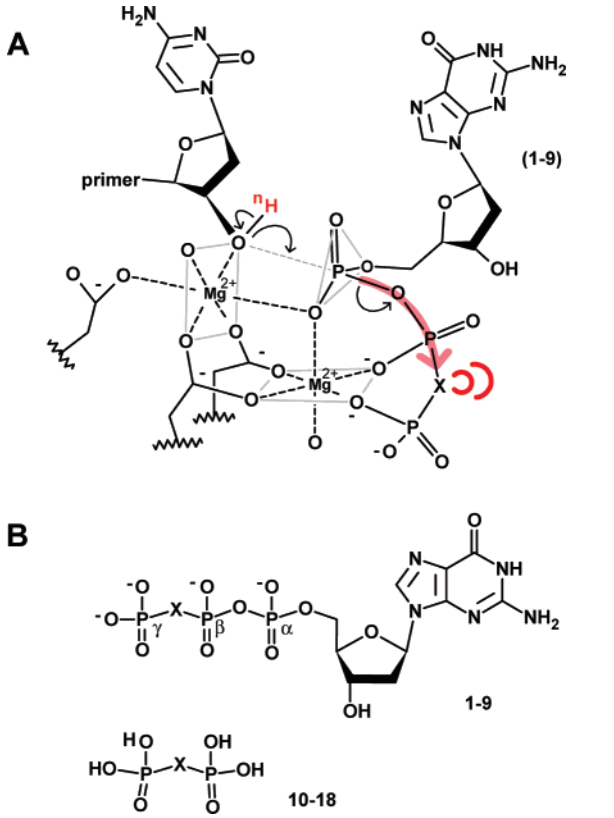

FIGURE 1: (A) Schematic diagram of the pol β active site based on atomic positions from crystal diffraction (*3*), showing the positions of the primer and incoming nucleotides, catalytic Mg^{2+} ions, and key aspartate residues. In this study the β-γ bridging triphosphate oxygen is replaced with a series of halomethylene groups, and the pH and solvent isotope content varied. Mechanistic effects on both correct (C-G) and mispair (T-G) incorporation in terms of substituent electron-withdrawing ability (indicated by rouge arrow) and other steric/electronic properties (indicated in rouge) at the β-γ bridging position or proton-exchangeable sites are examined. (B) Structures of dGTP and analogues, **1**−**9**, and bisphosphonic acids, **10**−**18**, prepared for kinetic and thermodynamic analysis. Compound numbers follow the trend in the substituent effect on pK_{a4} of the bisphosphonic acids (see Table 1). X = CF_2 (**1**, **10**); CFCl (**2**, **11**); CCl_2 (**3**, **12**); O (**4**, **13**); CHF (**5**, **14**); CBr_2 (**6**, **15**); CHCl (**7**, **16**); CHBr (**8**, **17**); and CH_2 (**9**, **18**).

EXPERIMENTAL PROCEDURES

Materials. High purity solution dGTP and T4 polynucleotide kinase (Optikinase) were purchased from GE Healthcare. DNA synthesis reagents and protected deoxyribonucleoside phosphoramidites were purchased from Applied Biosystems. Radiolabeled [γ-^{32}P]ATP was purchased from MP Biomedicals. The following deuterated reagents were purchased from Sigma-Aldrich: D_2O, DCl solution, TRIS-d_5, and glycer(ol-d_3) (98−99.9 atom % D). Other buffer components and chemicals for dGTP-analogue synthesis were purchased from Sigma-Aldrich or GE. Recombinant human WT pol β was expressed in *E. coli* and purified as described previously (*33*).

Synthesis of β-γ Bridging dGTP Analogues. Compounds were synthesized and characterized as described previously (*4*, *5*). Briefly, analogues of dGTP were prepared from dGMP morpholidate and the corresponding substituted-methylene-bisphosphonic acid, purified by two-stage preparative HPLC (>99%), and characterized by ^{1}H, ^{31}P, ^{19}F NMR and UV−visible spectra, analytical HPLC (Varian PureGel R00087E1PE

7 M 500A SAX), and negative ion FAB or MALDI HRMS. The monohalogenated analogues are diastereomeric; racemic mixtures of the *R* and *S* configuration at the β-γ bridging carbon were used in kinetic assays.

DNA Synthesis/Purification, Radiolabeling, and Annealing. Primer (TAT TAC CGC GCT GAT GCG C), template (GCG TTG TTC CGA C<u>M</u> G CGC ATC AGC GCG GTA ATA; <u>M</u> = C, T), and 5′-end-phosphorylated downstream (GTC GGA ACA ACG C) oligomers were synthesized on a solid-phase DNA synthesizer and purified as described previously (*5*). Primer DNA (1 mol equiv) was 5′-end labeled using T4 polynucleotide kinase (0.4 U/μL) and [γ-^{32}P]ATP (~0.7 mol equiv) using the supplied buffer. The kinase was inactivated after 30 min by heating at 90 °C for 10 min, and the reaction mixture was used for annealing without further purification. Annealing was carried out by mixing primer, template (1.2 mol equiv), and downstream (1.5 mol equiv) oligomers, heating to 90 °C, and then cooling slowly to room temperature.

Buffer Preparation. The assay buffers used to study dGTP or analogue incorporation kinetics consisted of 50 mM Tris-Cl, 20 mM KCl, 20 mM NaCl, 10 mM $MgCl_2$, 1 mM DTT, and 6 v/v % glycerol. Buffers were prepared at various acidities by adjustment with HCl or NaOH solution and monitoring pH with a Tris-compatible electrode. Deuterium-enriched buffer was prepared using deuterated Tris, glycerol, and D_2O. Acidity was adjusted with DCl solution according to the relation pD = (pH meter reading) + 0.4. All pH or pD values reported in the text were measured at 23 °C.

Single-Turnover Gap-Filling Assays. Single-nucleotide gapped DNA (template C or T) was preincubated for ~2 min at 37 °C with pol β in assay buffer and then mixed with a solution of substrate (dGTP or analogue in assay buffer at 37 °C). Concentrations after mixing were 300 nM pol β, 50 nM DNA, and 0.5−20 μM substrate (C-G incorporation) or 50−1500 μM substrate (T-G incorporation). The reaction mixture was quenched by ~3-fold dilution with 500 mM EDTA. Reaction time ranges were 0.09−0.5 s (C-G) and 0.5−100 s (T-G). Reaction times under 20 s were carried out with a rapid-mixing chemical quench apparatus (KinTek model RQF-3); otherwise, mixing was done manually with a micropipette. The radiolabeled 19-mer primer and 20-mer product were separated by denaturing polyacrylamide gel electrophoresis (39 × 33 × 0.035 cm, 20 w/v % polyacrylamide, 8 M urea gels run at 65 W, 4.5 h). Percentage of primer extended was measured by exposure of the dehydrated gel to a storage phosphor screen followed by detection of phosphorescence emission on an imaging system (Molecular Dynamics STORM 860). For β-γ bridging analogues and isotope work, three replicates were performed for each substrate/template base combination, and the best-fit values for k_{pol} and K_d are reported in Tables 1 and 2 as the mean ± standard error. The analogue assays were performed at a pH of 8.0. Assays performed in deuteronic solvent were performed at a pD of 8.6 and for calculation of the D_2O effect, were compared with data in protonic solvent at equivalent acidity (see Buffer Preparation).

Data Analysis. Kinetic assays were performed under single-turnover conditions ($E \gg S$) where the time evolution of product formation fits a single exponential: $[P]_t = [P]_{final}(1 - \exp[-k_{obs}t])$, where P is the extended primer product and k_{obs} is the observed catalytic rate constant. The observed rate constants were plotted against the substrate concentrations and the data fit to the hyperbolic equation: $k_{obs} = k_{pol}[S]/([S] + K_d)$, where S is dNTP substrate (dGTP or analogue), k_{pol} is an overall rate constant for the nucleotide insertion step(s), and K_d is the dissociation constant for substrate binding. The pH dependence of k_{pol} was fit to a sigmoidal function describing a single ionization: $k_{pol} = k_{lim}(1 + 10^{pKa-pH})^{-1} + k_o$; where k_{lim} and k_o define k_{pol} at the limits of pH. Fidelity for dGTP or analogue incorporation was calculated as $(k_{pol}/K_d)_{CG}/(k_{pol}/K_d)_{TG}$, where the subscripts refer to correct (C-G) and mispair (T-G) incorporation. The above terms can be rearranged to $(k_{pol,CG}/k_{pol,TG})$ $(K_{d,TG}/K_{d,CG})$, to reflect contributions from catalytic and binding terms, respectively.

Table 1: Kinetic and Thermodynamic Parameters for Incorporation of β-γ Bridging dGTP Analogues in Pol β-Catalyzed Single-Turnover Assays[a]

M-N	-X-	pK_a[c]	k_{pol} (s^{-1})	K_d (μM)	k_{pol}/K_d ($s^{-1}M^{-1}$) × 10^5	fidelity
C-G[b]	CF_2	7.8	21.9 ± 0.9	2.9 ± 0.3	75	
C-G	CFCl	8.4	14.9 ± 0.3	3.4 ± 0.5	44	
C-G	CCl_2	8.8	8.4 ± 1.0	3.7 ± 1.3	23	
C-G[b]	O	8.9	14.9 ± 2.3	1.7 ± 0.7	87	
C-G[b]	CHF	9.0	14.6 ± 2.3	2.2 ± 1.5	65	
C-G	CBr_2	9.3	3.1 ± 0.2	11.4 ± 1.4	2.7	
C-G	CHCl	9.5	8.1 ± 3.0	3.0 ± 1.7	27	
C-G	CHBr	9.9	6.9 ± 0.8	2.1 ± 0.2	33	
C-G[b]	CH_2	10.5	1.7 ± 0.2	0.9 ± 0.2	18	
T-G[b]	CF_2	7.8	0.76 ± 0.01	380 ± 50	0.020	3700
T-G	CFCl	8.4	0.23 ± 0.03	390 ± 80	0.0059	7600
T-G	CCl_2	8.8	0.05 ± 0.00	800 ± 70	0.00063	37000
T-G[b]	O	8.9	1.34 ± 0.10	200 ± 7	0.066	1300
T-G[b]	CHF	9.0	0.93 ± 0.06	270 ± 130	0.034	1900
T-G	CBr_2	9.3	0.02 ± 0.01	500 ± 200	0.00036	7600
T-G	CHCl	9.5	0.23 ± 0.03	410 ± 50	0.0056	4800
T-G	CHBr	9.9	0.14 ± 0.02	470 ± 130	0.0030	11000
T-G[b]	CH_2	10.5	0.12 ± 0.03	470 ± 110	0.0025	7100

[a] Assays were performed by rapid mixing chemical quench at a pH of 8.0 (23 °C). M-N is the template-incoming base-pair and -X- is the β-γ bridging group. Values of k_{pol} and K_d are reported as the mean ± standard deviation of three replicates, and error in the efficiencies (k_{pol}/K_d), and fidelity, $(k_{pol}/K_d)_{CG}/(k_{pol}/K_d)_{TG}$, are calculated according to the standard rules for error propagation. [b] Data from ref *5* used in average. [c] Bisphosphonic acid pK_{a4} values from ref *34*, pyrophosphoric acid pK_{a4} value from ref *51*.

Table 2: Kinetic and Thermodynamic Parameters for dGTP Incorporation in Protonic and Deuteronic Solvents[a]

M-N	solvent	k_{pol} (s^{-1})	K_d (μM)	D_2O effect
C-G	H_2O	22.0 ± 1.4	1.4 ± 0.2	3.7 ± 0.4
C-G	D_2O	6.1 ± 0.6	1.0 ± 0.1	
T-G	H_2O	2.0 ± 0.1	150 ± 46	6.6 ± 0.4
T-G	D_2O	0.3 ± 0.0	250 ± 29	

[a] Assays were performed by rapid mixing chemical quench at constant acidity (pD = pH = 8.6 at 23 °C). M-N is the template-incoming base-pair, and isotope-enriched buffer was prepared as described (see Buffer Preparation). The D_2O effect is calculated as the ratio $k_{pol,H}/k_{pol,D}$.

RESULTS

The use of dNTP analogues modified at the β-γ bridging oxygen as a probe of nucleotidyl-transfer mechanism has been demonstrated with pol β (*5*) using compounds having methylene and fluoromethylene groups (**1**, **5**, and **9** in Figure

1B). The analysis is now expanded to include halogenated moieties (**2**, **3**, **6**−**8**) at the β-γ bridging position having a more extensive set of steric and electronic properties. The conjugate acids of the respective pyrophosphate-like leaving groups (**10**−**18**) have also been prepared for systematic evaluation of their stability constants. Detailed procedures for the synthesis and purification of $O_{\beta\gamma}$-modified dNTP analogues and corresponding bisphosphonates are given elsewhere (*4*). Synthetic protocols and characterization data for compounds not previously reported appear in Supporting Information. Presently, our expanded set of $O_{\beta\gamma}$-modified dGTP analogues makes necessary the characterization of bisphosphonic acid protonation equilibria for heretofore unreported species, as well as the compilation of such values for the entire series under a set of identical, well-defined conditions for consistency in LFER determinations. Using the bisphosphonic acids **10**−**18** as analytes, potentiometric titrations for the series of compounds with KOH and identical conditions of temperature and ionic strength have been performed (*34*). These data are indicated in Table 1. The trend in pK_a values with the number of electronegative halogens on the bridging group, and a comparison with available literature values, is discussed elsewhere (*34*).

Pol β-Catalyzed Nucleotidyl Transfer Using $O_{\beta\gamma}$-Modified dGTP Analogues. Our primary objective in designing a series of halo-substituted dNTP analogues is to slow down or speed up the chemical step of leaving group elimination in order to probe its relative prominence in the overall scheme of nucleotidyl transfer. The LFER established with such a series of substrates is a well-known tool for deciphering reaction mechanisms in solution and in enzymatic reactions (*35*−*37*). In order to be effective in an LFER analysis, the $O_{\beta\gamma}$ modification must alter the activation barrier for $P_\alpha-O_{\alpha\beta}$ bond breaking and the subsequent product state to the exclusion of other local transition or ground states along the reaction coordinate, including any conformational states involving protein or DNA moieties. Key evidence in favor of these assumptions is that X-ray crystal structures of the CH_2 and CF_2 analogues in ternary complex with pol β and DNA are in excellent overlap with the conformation of native dNTP, and catalytic active-site components are properly aligned (*5*); K_d data on previously assayed analogues are also comparable with native dNTP binding (*5*). Despite these positive assertions, implications of the previous work on $O_{\beta\gamma}$ modification rested on relatively few analogues between the extremes of leaving group acidity (i.e., between CF_2 and CH_2 analogues). In this work we increase the number of interpolating points from two to seven, varying charge and size, so as to arrive at new and more general mechanistic insights.

Single-turnover transient kinetic assays of pol β-catalyzed incorporation of analogues **2**, **3**, **6**−**8** into 1-nt gapped DNA were performed in a standard manner by rapid mixing chemical quench. Two different template DNA strands were studied (templating base C or T). At least three independent trials were performed with each analogue to obtain the parameters k_{pol} and K_d, the overall catalytic rate and dNTP dissociation constants, respectively. These parameters are shown in Table 1 (Figure S1 in Supporting Information depicts the result of a typical assay). Brønsted plots are shown in Figure 2 according to the relation $\log(k_{pol}) = \beta_{lg}(pK_{a4}) + C$. The constant β_{lg} is a measure of the sensitivity

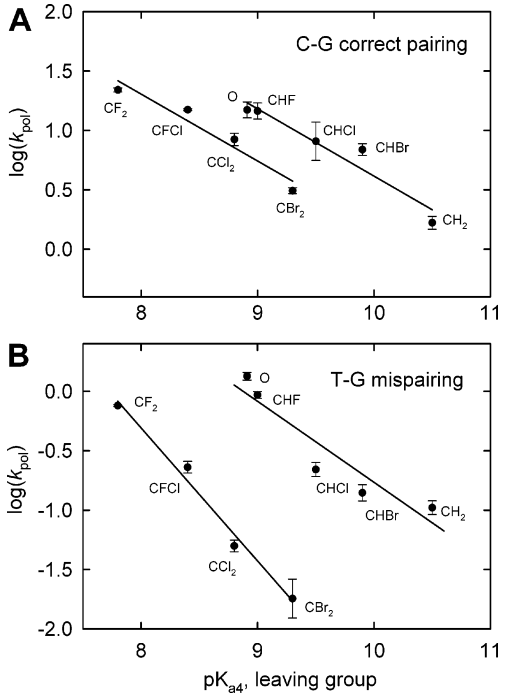

FIGURE 2: Brønsted correlations of log(k_{pol}) versus leaving-group pK_{a4}. Data for dGTP and analogues, **1**−**9**, incorporated opposite (A) the correct template base C, and (B) the mispairing template base T. For both C-G and T-G graphs, the data for monohalogenated analogues, the methylene analogue, and native dGTP conform to a linear relationship between pK_{a4} 9−11 ($\beta_{lg,CG} = -0.56$ and $\beta_{lg,TG} = -0.68$). The catalytic sensitivity to leaving group ability in this region is similar to that reported for other enzymatic P−O bond cleavages (*32*, *50*) and suggests leaving-group elimination is rate-limiting (or near rate-limiting) for incorporation of dGTP opposite either template. The di-halogenated analogues (connected by separate solid lines, with $\beta_{lg,CG} = -0.56$ and $\beta_{lg,TG} = -1.12$) show deviation from the other data which is more pronounced for incorporation of the mispair.

of k_{pol} to leaving group ability, and C (the intercept) is a constant of no physical significance.

Kinetics of Correct-Base Incorporation: dGTP Analogues Opposite Template Base C. The chief finding of our earlier work (*5*) primarily with fluoromethylene bridging groups was a biphasic LFER suggesting a change in rate-limiting step due to modification at $O_{\beta\gamma}$; the position for the oxo-bridging compound near the apparent intersection of two linear regions suggested that for the natural dNTP two or more activation barriers lie approximately equal in height on the reaction coordinate. The present work adds interpolating points to the Brønsted plot for incorporation opposite template C that allows for more detailed evaluation (Figure 2A).

First, the monohalogenated compounds studied now comprise CHBr, CHCl, and CHF groups. Data points for these compounds fall between the O and CH_2 analogue points and are colinear. The β_{lg} calculated for the region between pK_{a4} 9−11 is relatively steep, −0.56, consistent with significant contribution of the elimination step to the rate-limiting transition state. Second, the recent pK_a study of bisphosphonic acids (*34*) indicates that Claessens's pK_{a4} value for the CCl_2 analogue (*38*), upon which we relied in our previous work (*5*), is high by about 1 unit; we have adjusted this value to 8.8 as shown in Figure 2. At a pK_{a4} of 9.7 the CCl_2 analogue position fell colinear with that for O, CHF, and CH_2 compounds; with the present value, that better

represents the trend in halo-substitution (*34*), this point now deviates from the rightmost line in Figure 2A, as does that for the bulky CBr_2-bridging compound. Additionally, the points for the CF_2 and CFCl analogues deviate in the same direction (reduction in k_{pol} relative to a single linear trend).

The systematic reduction in catalytic activity with dihalogen-substituted analogues raises the possibility that steric properties may affect k_{pol}, and the log(k_{pol}) vs pK_{a4} data for these compounds, suggesting that they may more appropriately be treated separately from the others. Although the deviation between the linear relationships drawn for the dihalogen compounds (leftmost line in Figure 2A) and the others (rightmost line) appears modest, such separate treatment will be justified when the kinetics of mispair incorporation are considered below.

The K_d values for binding with the new analogues (Table 1) confirm previous structural and binding equilibrium data suggesting that a wide range of halomethylene groups are accepted at the β-γ bridging position with minimal perturbation of substrate binding. For incorporation opposite template C the K_d values, with the exception of the CBr_2 analogue, fall in the narrow range 1−4 μM, in excellent agreement with that of native dGTP.

Kinetics of Mispair Incorporation: dGTP Analogues Opposite Template Base T. Prior to expanding the series of β-γ bridging analogues to include chloro-, bromo-, and mixed-halomethylene groups, the shape of Brønsted correlations for C-G and T-G incorporation appeared similar both in β_{lg} in the catalytically sensitive region and in the position of the break in the biphasic plots (*5*), suggesting that both processes, i.e., right compared with wrong incorporations, are catalyzed via similar rate-limiting chemical steps, as opposed to a dominant conformational change barrier. Here, we find that addition of points for the expanded set of analogues affirms that a catalytically sensitive linear region exists at p$K_{a4} \geq 9$ ($\beta_{lg} = -0.68$). The considerably diminished activity for dihalogen compounds opposite template T, however, underscores important differences between correct and mispair incorporation mechanisms.

While the kinetics of the monohalogenated analogues put their respective points tightly colinear with those of O- and CH_2 compounds (Figure 2B), as was the case in Figure 2A, the new dihalogenated analogues (CFCl, CCl_2, CBr_2-) show deviations to a significantly greater extent than observed in correct base incorporation, again presumably due at least in part to the increased steric bulk of the halogen substituents. This is illustrated by comparing dihalogen lines with the rightmost lines in each of Figures 2A and 2B. The trend in the dihalogen data, besides showing diminished activity, is linear and parallel to the rightmost line in Figure 2B. Invoking a "dihalogen correction factor" could reconcile all points onto a single LFER line, by shifting the dihalogen points upward, but the physical basis for such a correction is not well defined. If plausible, it would suggest that the LFER behavior of T-G mispair incorporation, after steric correction, would extend with negative slope over the entire pK_{a4} range shown and not exhibit a break in linearity near the pK_{a4} of the native pyrophosphoric acid. The same procedure could in principle be applied to the correct incorporation plots in Figure 2A, with the same result albeit with smaller presumed correction factor.

In a theoretical model, if the activation barrier to leaving group elimination is sufficiently high relative to other barriers near the transition state, perturbation of its height (i.e., by $O_{\beta\gamma}$ modification) would result in a single linear plot in the LFER formalism. On the other hand, if the leaving group elimination barrier lies close in height to its neighbors, sufficient stabilization (at the far left of Figures 2A and 2B) would be predicted to result in a break in linearity with a catalytically insensitive (zero slope) region at low leaving group pK_a. Reconciling the experimentally observed plots with either theoretical model (single line versus biphasic) is difficult, even with the expanded set of halomethylene bridging analogues, because the CF_2 bridging species remains the strongest leaving group, and in both correct and T-G mispairing incorporation its point falls roughly level with that of the native compound, so a biphasic model profile cannot be ruled out. Regardless of theoretical model, the significantly stronger dihalogen-dependent reduction in catalysis for T-G mispairing suggests energetic and structural differences compared to correct incorporation.

The K_d values for analogues in mispair assays (Table 1) do not show the same trend in deviation as observed for log(k_{pol}). The CCl_2 analogue has a K_d approximately 4-fold higher than that of dGTP, but those for CBr_2 and CFCl analogues are no higher than K_d values for monohalogenated analogues. Therefore, the differences implied by Figure 2 likely occur at the chemical transition state as opposed to the conformational activation barriers preceding the formation of the bound ternary complex. The intermolecular steric/electrostatic effects may be triggered as small geometric distortions, propagated from the base moiety of the mispair to the catalytic site (*39*). Possible origins of this catalytic difference will be explored further in the Discussion.

Effect of $O_{\beta\gamma}$ Modification on Fidelity. Fidelity in this work is computed as the ratio of catalytic efficiencies (k_{pol}/K_d) for substrates with the same nucleobase (dGTP or analogue), opposite two different template bases, C or T. This "template-variable" fidelity (Table 1) contrasts with polymerase selectivity *in vivo*, where four different nucleobases compete for incorporation opposite the same template base. Since the environment of the template base and that of the dNTP are different in the active site, selectivity measured by template-variable fidelity may not be the same as the *in vivo* process. In either case, however, the enzyme preferentially catalyzes the correct-pairing reaction, so template-variable fidelity is a valid measure of polymerase mechanism. Reckoning fidelity in this manner allows for comparison with computational simulations and facilitates further computational analysis of $O_{\beta\gamma}$ modifications, where a template-variable model is adopted to minimize inaccuracies in calculated parameters (*5*, *40*).

Our results with the expanded series of halomethylene analogues indicate that overall, $O_{\beta\gamma}$ modification results in an increase in fidelity for T-G mispair incorporation (roughly 27-fold for the CCl_2 analogue). The strongest enhancement in discrimination is a direct result of the large reduction in k_{pol} for incorporation of the mispair with the dihalogen-substituted compounds. This enhancement is further illustrated in Figure 3, where the separate catalytic ($k_{pol,CG}/k_{pol,TG}$) and binding ($K_{d,TG}/K_{d,CG}$) contributions to fidelity are graphed. The strong effect on pol β fidelity with the CCl_2 analogue is due to a favorable catalytic contribution. Because of its

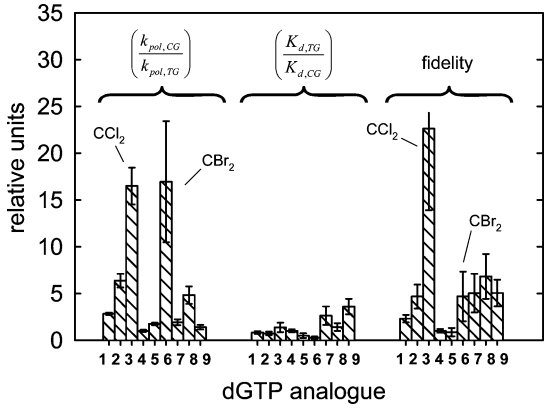

FIGURE 3: Effect of $O_{\beta}\gamma$ modification on fidelity. The k_{pol} and K_d ratios (discussed in the text) for each analogue are plotted relative to that of native dGTP and account for contributions to fidelity (right) from catalysis and substrate binding, respectively. Error bars are calculated by propagation of error in the corresponding k_{pol} and K_d terms. The dominant effect is a roughly 27-fold increase in fidelity for the CCl_2 analogue due to marked reduction in k_{pol} for mispair incorporation. Surprisingly, an equal-or-greater effect is not observed with the CBr_2 analogue despite a favorable k_{pol} ratio. This can be explained by relatively poor binding of the CBr_2 analogue opposite the correct template base C.

poor binding opposite template C, the CBr_2 analogue does not have the strongest effect on fidelity, even though its catalytic term is larger than that of the CCl_2 compound.

The roughly 27-fold increase in fidelity for the CCl_2 analogue is notable, considering that the leaving group for this substrate, compound **10**, is one of the most investigated of the bisphosphonate class of drugs (clodronate), used clinically for over 15 years in the treatment of hypercalcemia and bone metastases (*41*, *42*). Simple bisphosphonates, those that closely resemble pyrophosphate, are thought to act via intracellular conversion into β-γ bridging analogues of ATP, which are likely inhibitors of ATP-utilizing enzymes (*41*). To our knowledge there is no documentation of "simple" bisphosphonate conversion to the analogous *deoxy*-ribonucleotide substrates in humans, so the potential for clodronate targeting polymerase activity in human cells remains to be demonstrated, despite the significant effect observed here when clodronate is synthetically linked to dGMP.

The pH Dependence of Pol β Catalysis. Results presented here and in other studies (*6*, *25*) point to chemical steps as the rate-limiting barriers in pol β-catalyzed nucleotidyl transfer, as opposed to conformational changes subsequent to dNTP binding. One aspect of the chemical steps, proton transfer, is experimentally a relatively unexplored avenue in the pol β mechanism. Having investigated changes in bonding about P_{α}, we sought to characterize the pH dependence of pol β catalysis for both the C-G and T-G incorporation reactions, as a means of exploring chemistry antecedent to leaving group elimination.

Using the rapid chemical quench assay, k_{pol} and K_d parameters were obtained for incorporation of dGTP into the same DNA constructs used with the β-γ analogues. Reactions were performed at incremental pH values in the range 6.5−9.5 by adjusting the acidity of assay buffer; ionic strength was allowed to increase concomitantly. Control experiments in buffers with varying pK_as confirmed that for single turnovers at low DNA concentration the buffer capacity of Tris is sufficient in the pH range studied here

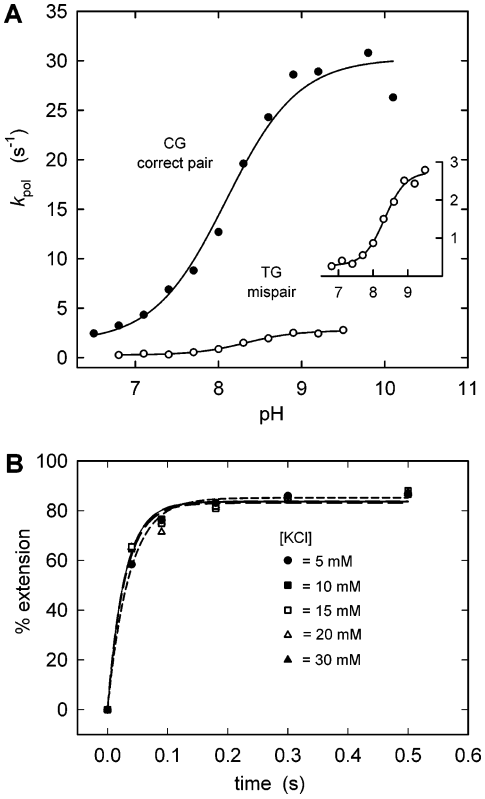

FIGURE 4: The pH dependence of pol β catalysis. (A)Values for k_{pol} were obtained for dGTP incorporation opposite either template base C (filled circles) or template base T (open circles) using rapid mixing chemical quench assays at the pH values indicated. Inset: pH profile for mispair incorporation shown at expanded scale. Solid lines show fits of the data to a sigmoidal function, yielding effective pK_as of 8.1 (C-G incorporation) and 8.4 (T-G incorporation). Measurement beyond pH ~ 9.5 was not reliable due to diminished pol β activity under these conditions. (B) Time courses for primer extension at constant pH and varying ionic strength. Rapid mixing chemical quench assays were performed under conditions of saturating dGTP concentration, where $k_{obs} \approx k_{pol}$. Ionic strength was varied by addition of KCl to the concentrations indicated; other buffer components remained at the same concentration. The data indicate that k_{pol} is insensitive to changes in ionic strength over this range, suggesting sensitivity to pH is due specifically to shifts in proton equilibria.

(Figure S2, Supporting Information). The k_{pol} values as a function of pH are plotted in Figure 4A. The control experiment where ionic strength was varied over the same range at constant pH by addition of KCl showed no change in the observed catalytic rate constant at saturating dGTP concentration (Figure 4B); therefore, the pH sensitivity of pol β catalysis is due specifically to shifts in proton equilibria rather than a more general ionic strength effect. A sigmoidal curve is observed with an apparent pK_a of 8.1 or 8.4 for incorporation of dGTP opposite either template base C or T, respectively (Figure 4A). Recently, the pH dependence of an RNA-dependent RNA polymerase with Mg^{2+} as cofactor has been shown to exhibit bell-shaped behavior suggestive of two proton-transfer events in the pH range 6−10 (*43*). The reverse-sigmoidal transition at higher pH may be attributed to protonation of the leaving group. Whether or not an analogous "reverse" transition at high pH occurs for pol β could not be determined because of the lack of activity beyond the pH range studied here. The single inflections observed (Figure 4A) may be assigned to the pK_a of primer 3′ OH deprotonation in the pol β active site,

assuming that acid/base equilibria of other groups do not contribute to the pH dependence curve (*44*) near the inflection point. However the slope of the log(k_{pol}) versus pH profile is somewhat less than 1 (~0.75 for the C-G assay, data not shown), so the inflection points may not reflect a single macroscopic pK_a that is being titrated. The dissociation constant, K_d, for dGTP opposite either template shows little response as a function of pH, remaining flat over the same range (Table S1, Supporting Information).

The Solvent Deuterium Isotope Effect on Pol β Catalysis. Since the k_{pol} sensitivity to pH changes reflects changes in reaction equilibria but not in transition state energetics, we augmented these experiments by measuring deuterium solvent isotope effects. Table 2 shows rapid chemical quench data collected in protonic or deuteronic media at equivalent acidity (pH = pD). The D_2O effect ($k_{pol,H}/k_{pol,D}$) is large for both C-G and T-G incorporation (between 4 and 7). As with pH dependence, because many hydrogen bonds and acid/base equilibria are affected by the H/D exchange, unambiguous assignment of the deuterium kinetic isotope effect to a single proton transfer is difficult. Nevertheless, a similarity of the observed magnitude of this effect for pol β and four diverse classes of polymerases, including RNA and DNA dependent RNA and DNA polymerases (*7*, *43*), suggests a dominant contribution of hydrogen bonds that are present in the catalytic sites of all polymerases. Since these polymerases differ in the nature of the protein active site residues, hydrogen bonds involving the 3′-OH group on the primer or dNTP substrate, and hydrogen bonds between the substrate and template, may be significant. We find the solvent deuterium isotope effect is larger for T-G mispair incorporation, suggesting that perhaps primer, substrate, or template conformational changes during the chemical reaction occur along different pathways or have different magnitudes for correct versus incorrect insertions. The isotope effect could perhaps be explored profitably by a quantum classical path treatment (*45*).

DISCUSSION

X-ray crystal diffraction studies of pol β in various liganded states (*1*, *3*, *17*−*19*), begun over a decade ago, have provided the structural insight as to how protein residues could facilitate conformational changes and the chemical steps of nucleotidyl transfer. Recent structures obtained with nonhydrolyzable dNTP analogues (*3*) that allow the crucial primer 3′ OH and Mg^{2+} ions to be retained largely confirmed and extended the earlier findings employing abortive dideoxy-terminated substrates (*17*). In terms of geometry near the site of chemical steps (Figure 1A), the nucleotide-binding Mg^{2+} coordinates nonbridging oxygens on all three phosphates of the correct incoming dNTP (α,β,γ tridentate), whereas the other, so-called "catalytic" Mg^{2+}, coordinates the same nonbridging oxygen on P_α and directly coordinates the primer 3′ oxygen, activating it for in-line nucleophilic attack. The implication of the Mg^{2+} coordination scheme depicted in Figure 1A is that the negative charge developing on $O_{\alpha\beta}$ is not directly stabilized by coordination with either metal cation. Moreover, inspection of high-resolution crystal structures shows no amino acid residue likely to provide such stabilization (*18*). It is important to emphasize that these structural findings regarding conformational changes and the positioning of active site participants are limited to Watson−Crick nascent base pairs. Ternary pol−DNA−dNTP complexes, which provide structural information that is currently the most relevant to the chemical transition state (in the absence of a transition state analogue structure), remain an elusive target when the nascent base pair does not conform to Watson−Crick base pairing (*20*), impeding efforts to characterize the insertion mechanism of base substitution errors.

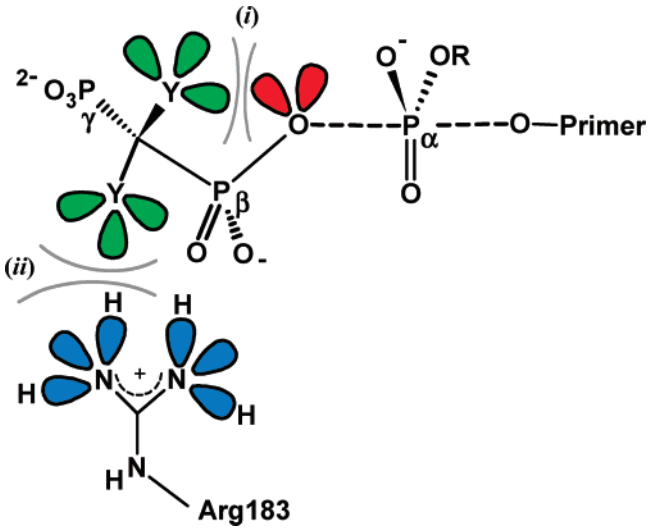

FIGURE 5: An illustration of possible interactions at the chemical transition state, between bulky halogen atoms at the β-γ bridging position (atoms labeled Y) and other elements of the active site. Repulsion between the pro-*S* halogen and $O_{\alpha\beta}$, labeled (*i*), or a catalytically debilitating steric/electrostatic interaction between the pro-*R* halogen and Arg183, labeled (*ii*), may be more pronounced in the mispair, indicative of active-site differences at the chemical transition state.

The primary motivation for applying LFER methodology to leaving group elimination in the pol β system is to establish a direct probe of the energetics of the chemical steps of nucleotidyl transfer, and to potentially distinguish between different models of LFER behavior which relate the height of leaving group elimination barriers to other steps in the pathway. The diminished catalytic activity observed for bulky dihalogen-bridging analogues, with greater magnitude for T-G mispair incorporation compared to C-G incorporation, was unexpected. This observation complicates interpretation of the experimental LFERs of Figure 2 in terms of ideal model behavior but offers an opportunity to infer active site differences between correct and mispair incorporation from a perspective unavailable from X-ray crystallography alone.

Figure 5 is a schematic diagram of the chemical transition state for nucleotidyl transfer. Two possible interactions between β-γ bridging group halogens and active-site atoms are illustrated in Figure 5, which may account for the diminished activity observed with bulky dihalogen atoms and the different behavior between correct and mispairing assays at the transition state.

First, intramolecular repulsion between the negative charge developing on $O_{\alpha\beta}$ and the pro-*S* halogen may hinder leaving group elimination. All-atom empirical valence-bond/free-energy perturbation (EVB/FEP) simulations in pol β and aqueous solution carried out for incorporation of the CF_2 analogue (*5*) suggested heightened chemical activation barriers for this compound with contributions from intramo-

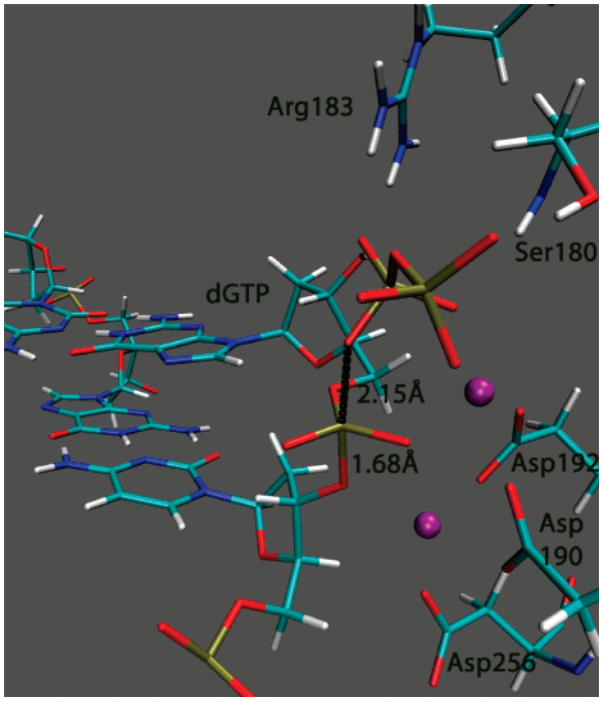

FIGURE 6: Average EVB/FEP geometry of the rate-limiting transition state for the chemical reaction catalyzed by pol β (*5*). This transition state corresponds to a calculated Brønsted β_{lg} of −0.73. Bond lengths shown correspond to P_α−O3 (1.68 Å) and P_α−$O_{\alpha\beta}$ (2.15 Å).

lecular steric and electrostatic repulsion involving $O_{\alpha\beta}$ and one of the two fluorine atoms. Since this contribution, labeled (*i*) in Figure 5, is larger in the transition state than in the reactant state, it may cause the diminished catalytic activity observed for the dihalogen compounds. Upon going from F to larger but less electronegative Cl and Br atoms, we expect the electrostatic repulsion to decrease and steric repulsion to increase. This offsetting trend may explain the small dependence of the dihalogen effect on the van der Waals size of the halogen atom and the good fits to linearity for dihalogen-bridging compounds in Figure 2.

Theoretical analyses have indicated that the LFER for phosporyl transfer reactions are expected to be similar in enzymes and in solutions as long as the rate-limiting steps are similar (*46*, *47*), regardless of the structural details of the enzyme active site. Although anomalous behavior when, for example, product states containing negatively charged leaving groups with lower pK_a would be less stable than groups with higher pK_a cannot be completely excluded, the fact that pol β active-site structure shows the absence of any metal cation or enzyme group capable of directly stabilizing the negative charge that develops on $O_{\alpha\beta}$ during leaving group elimination (*18*) greatly reduces the chance of such anomaly by eliminating quantum chemical effects associated with strong hydrogen bonding or metal−ligand complexes. Thus, we expected to observe a LFER with a slope similar to the slope observed in model diester hydrolysis reactions in aqueous solution (*34*−*37*). Since this LFER is obtained, it is likely that P−O bond breaking contributes significantly to the rate-limiting step. Steep LFER slopes for both correct and incorrect incorporation suggest similar positions of the chemical transition state (Figure 6) on the free energy surface, although β_{lg} values for the T-G mispair assay are somewhat higher than for correct pairing (see Figure 2), suggesting a higher degree of P_α−$O_{\alpha\beta}$ bond breaking in the transition state of the mispair.

A second possibility, not mutually exclusive of intramolecular repulsion with $O_{\alpha\beta}$, is that a steric/electrostatic interaction between the pro-*R* halogen and the nearby guanidino group of Arg183 is catalytically debilitating; labeled (*ii*) in Figure 5. Arg183 forms an H-bond with the β phosphate in correct incorporation of natural dNTPs and plays an important role in transition state stabilization (*48*); the presence of additional negative charge density nearby, in the form of the pro-*R* halogen, may interrupt this transition state stabilization. Recently, it has been shown that a stereospecific pol β ternary complex forms with the *R* isomer of the CHF analogue (**5**), despite both *R* and *S* isomers being present in the crystallization mixture (*4*), suggesting the *R* isomer is stabilized by a preferential H−F interaction with Arg183. The precise nature of interactions between Cl or Br atoms and the Arg183 guanidino group is unknown, as ternary crystal structures with CCl_2- or CBr_2-bridging analogues are yet to be reported.

The same interactions described above and in Figure 5 may also occur to some extent with the monohalogenated analogues. The finding that catalysis is severely diminished for dihalogenated species, whereas monohalogenated compounds are collinear with non-halogenated O and CH_2 bridging compounds, may suggest that only when a combination of halo effects from both the pro-*R* and pro-*S* positions are present is the LFER perturbed.

The report of stereospecific pol β ternary complex formation with the *R* isomer of the CHF analogue (*4*), under crystallization conditions, also raises the question whether an analogous preference for the *R* isomer occurs under conditions of our kinetic assays, since the monohalogenated analogues used here are racemic mixtures of the *R* and *S* configurations at the β-γ bridging position. Interestingly, while the CHF bridging group shows a stereospecific preference under crystallization conditions, the CHCl and CHBr groups do not (*4*). Careful inspection of the time courses and saturation curves for primer extension (Figure S1, Supporting Information) can also provide limited clues as to the behavior of the two diastereomers. That K_d data for monohalogenated analogues opposite template C fall in the same narrow range as dihalogenated analogues and the native dGTP, and time courses giving k_{obs} are good fits to single exponentials rather than double exponentials, argues against very large differences in binding or catalysis behavior for the *R* versus *S* configuration under the reaction conditions used for this work. This does not exclude the possibility that more subtle differences between isomers exist. The availability of pure diastereomers (requiring a clever strategy for purification of diastereomeric dNTP analogues or chiral bisphosphonate derivatives) would help resolve this question.

In addition to studying LFER behavior as a function of leaving group acidity, the dependence of pol β-catalyzed nucleotidyl transfer on pH and solvent deuterium isotope content was evaluated to determine the extent to which proton transfers can affect the rate. We find both C-G correct and T-G mispairing reactions to be sensitive to pH and to exhibit a large kinetic isotope effect (KIE), indicative of proton-transfer steps as partially rate limiting along with leaving group elimination. In a recent study using an RNA-dependent

RNA polymerase (RdRp), Castro et al. (*43*) interpreted the nonlinear proton-inventory plots measured in mixed H_2O/D_2O solvents as evidence for two proton transfers at the chemical step. A large solvent deuterium isotope in this system (KIE = 7) suggested chemistry proceeds through a highly symmetrical transition state with proton transfers from primer 3′ OH and to pyrophosphate occurring in a coordinated fashion.

Our finding of both an appreciable KIE and catalytic sensitivity to leaving group acidity is consistent with a concerted mechanism in pol β, with significant contribution from proton transfer from the 3′ O−H bond, and both $O_{3'}-P_\alpha$ bond making and $P_\alpha-O_{\alpha\beta}$ bond breaking at the transition state. The large magnitude of the deuterium KIE may be due in part to a change in the pK_a of the 3′-OH group of the nucleophile in D_2O. It is also possible that the strength of H-bonds other than those involving the nucleophile change upon going from the ground state to the transition state, contributing to the KIE.

In particular, a larger kinetic deuterium effect for the T-G mispair may be explained if we attribute the kinetic deuterium effect to the presence of a strong intramolecular hydrogen bond between the 3′OH group of dGTP and one of its nonbridging β-phosphate oxygen atoms (Figure 6). If the position of Arg183, which shares the H-bond acceptor atom with the 3′OH group, is shifted from its optimal position in the transition state due to the formation of the TG mispair, the intramolecular hydrogen bond becomes stronger in the same transition state, yielding a larger deuterium kinetic effect. The postulated effect of the 3′OH intramolecular hydrogen bond can be verified or excluded by measuring kinetic deuterium effects for ddGTP substrates.

The probes of nucleotidyl transfer chemistry described here have been used in the pol β system to separately evaluate the chemical steps of correct and mispair incorporation. The catalytic sensitivity to all three methods (LFER, pH, and KIE) is observed for both correct and mispair incorporation, providing evidence that chemical steps as opposed to conformational rearrangements are the rate limiting steps. The magnitude of diminished activity using dihalogenated leaving groups, dependent on the identity of the template base, is a key finding. While the origins of the observed dihalogen effect on nucleotidyl transfer mechanism cannot be determined by the present work alone, this finding and future work with other functional groups introduced at the β-γ bridging position may help to identify important structural differences in transition states for correct and mispair incorporation and to suggest future protein active-site mutagenesis experiments and computer simulations that can be used to verify and refine hypotheses on the nature of structural differences. The fidelity of pol β is intermediate between the highly accurate replicative polymerases and the most error-prone (*49*); further progress in understanding nucleotidyl transfer mechanism may therefore come in applying the methodology described here to other polymerases and to other combinations of nascent base pairs including mispairs less stable than the relatively facile T-G mispair.

ACKNOWLEDGMENT

The authors thank Drs. George Kenyon, Steve Benkovic, and David Gorenstein, who have provided their expertise serving as active scientific overseers for our Program Project on DNA polymerase fidelity mechanisms. The authors also thank Dr. Václav Martínek for many helpful discussions.

SUPPORTING INFORMATION AVAILABLE

Synthetic protocols and characterization data for novel dGTP analogues. Time courses and rate saturation curve for incorporation of dGTP(β,γ)CHBr opposite template base C. Time courses for dGTP incorporation opposite template C in different buffers at low and high pH. Tabulated values of k_{pol} and K_d for incorporation of dGTP opposite template bases C and T at pH values between 6.5 and 9.5. This material is available free of charge via the Internet at http://pubs.acs.org.

REFERENCES

1. Batra, V. K., Beard, W. A., Shock, D. D., Pedersen, L. C., and Wilson, S. H. (2005) Nucleotide-induced DNA polymerase active site motions accommodating a mutagenic DNA intermediate, *Structure 13*, 1225−1233.
2. Batra, V. K., Shock, D. D., Prasad, R., Beard, W. A., Hou, E. W., Pedersen, L. C., Sayer, J. M., Yagi, H., Kumar, S., Jerina, D. M., and Wilson, S. H. (2006) Structure of DNA polymerase beta with a benzo[c]phenanthrene diol epoxide-adducted template exhibits inutagenic features, *Proc. Natl. Acad. Sci. U.S.A. 103*, 17231−17236.
3. Batra, V. K., Beard, W. A., Shock, D. D., Krahn, J. M., Pedersen, L. C., and Wilson, S. H. (2006) Magnesium-induced assembly of a complete DNA polymerase catalytic complex, *Structure 14*, 757−766.
4. McKenna, C. E., Kashemirov, B. A., Upton, T. G., Batra, V. K., Goodman, M. F., Pedersen, L. C., Beard, W. A., and Wilson, S. H. (2007) (*R*)-β,γ-fluoromethylene−dGTP−DNA ternary complex with DNA polymerase beta, *J. Am. Chem. Soc.* (in press).
5. Sucato, C. A., Upton, T. G., Kashemirov, B. A., Batra, V. K., Martinek, V., Xiang, Y., Beard, W. A., Pedersen, L. C., Wilson, S. H., McKenna, C. E., Florián, J., Warshel, A., and Goodman, M. F. (2007) Modifying the beta,gamma leaving-group bridging oxygen alters nucleotide incorporation efficiency, fidelity, and the catalytic mechanism of DNA polymerase β, *Biochemistry 46*, 461−471.
6. Bakhtina, M., Lee, S., Wang, Y., Dunlap, C., Lamarche, B., and Tsai, M. D. (2005) Use of viscogens, dNTPaS, and rhodium(III) as probes in stopped-flow experiments to obtain new evidence for the mechanism of catalysis by DNA polymerase β, *Biochemistry 44*, 5177−5187.
7. Bakhtina, M., Roettger, M. P., Kumar, S., and Tsai, M. D. (2007) A unified kinetic mechanism applicable to multiple DNA polymerases, *Biochemistry 46*, 5463−5472.
8. Beard, W. A., Shock, D. D., and Wilson, S. H. (2004) Influence of DNA structure on DNA polymerase beta active site function: Extension of mutagenic DNA intermediates, *J. Biol. Chem. 279*, 31921−31929.
9. Martinek, V., Bren, U., Goodman, M. F., Warshel, A., and Florián, J. (2007) DNA polymerase beta catalytic efficiency mirrors the Asn279-dCTP H-bonding strength, *FEBS Lett. 581*, 775−780.
10. Oelschlaeger, P. M. K. W. A. B. S. H. W. and Warshel, A. (2007) Magnesium-cationic dummy atom molecules enhance representation of DNA polymerase beta in molecular dynamics simulations: Improved accuracy in studies of structural features and mutational effects, *J. Mol. Biol. 366*, 687−701.
11. Lin, P., Pedersen, L. C., Batra, V. K., Beard, W. A., Wilson, S. H., and Pedersen, L. G. (2006) Energy analysis of chemistry for correct insertion by DNA polymerase beta, *Proc. Natl. Acad. Sci. U.S.A. 103*, 13294−13299.
12. Yang, L., Beard, W. A., Wilson, S. H., Broyde, S., and Schlick, T. (2002) Polymerase beta simulations suggest that Arg258 rotation is a slow step rather than large subdomain motions per se, *J. Mol. Biol. 317*, 679−699.
13. Beard, W. A., and Wilson, S. H. (1998) Structural insights into DNA polymerase beta fidelity: hold tight if you want it right, *Chem. Biol. 5*, R7−R13.
14. Hitomi, K., Iwai, S., and Tainer, J. A. (2007) The intricate structural chemistry of base excision repair machinery: Implica-

tions for DNA damage recognition, removal, and repair, *DNA Repair 6*, 410−428.
15. Lang, T. M., Maitra, M., Starcevic, D., Li, S. X., and Sweasy, J. B. (2004) A DNA polymerase beta mutant from colon cancer cells induces mutations, *Proc. Natl. Acad. Sci. U.S.A. 101*, 6074−6079.
16. Wang, L. M., Patel, U., Ghosh, L., and Banerjee, S. (1992) DNA polymerase beta mutations in human colorectal cancer, *Cancer Res. 52*, 4824−4827.
17. Sawaya, M. R., Prasad, R., Wilson, S. H., Kraut, J., and Pelletier, H. (1997) Crystal structures of human DNA polymerase beta complexed with gapped and nicked DNA: Evidence for an induced fit mechanism, *Biochemistry 36*, 11205−11215.
18. Pelletier, H., Sawaya, M. R., Wolfle, W., Wilson, S. H., and Kraut, J. (1996) Crystal structures of human DNA polymerase β complexed with DNA: Implications for catalytic mechanism, processivity, and fidelity, *Biochemistry 35*, 12742−12761.
19. Arndt, J. W., Gong, W. M., Zhong, X. J., Showalter, A. K., Liu, J., Dunlap, C. A., Lin, Z., Paxson, C., Tsai, M. D., and Chan, M. K. (2001) Insight into the catalytic mechanism of DNA polymerase β: Structures of intermediate complexes, *Biochemistry 40*, 5368−5375.
20. Beard, W. A., and Wilson, S. H. (2006) Structure and mechanism of DNA polymerase β, *Chem. Rev. 106*, 361−382.
21. Krahn, J. M., Beard, W. A., and Wilson, S. H. (2004) Structural insights into DNA polymerase beta deterrents for misincorporation support an induced-fit mechanism for fidelity, *Structure 12*, 1823−1832.
22. Xiang, Y., Goodman, M. F., Beard, W. A., Wilson, S. H., and Warshel, A. (2007) Exploring the role of large conformational changes in the fidelity of DNA polymerase beta, *Proteins 70*, 231−247.
23. Florián, J., Goodman, M. F., and Warshel, A. (2005) Computer simulations of protein functions: Searching for the molecular origin of the replication fidelity of DNA polymerases, *Proc. Natl. Acad. Sci. U.S.A. 102*, 6819−6824.
24. Beard, W. A., and Wilson, S. H. (2003) Structural insights into the origins of DNA polymerase fidelity, *Structure 11*, 489−496.
25. Dunlap, C., and Tsai, M. D. (2002) Use of 2-aminopurine and tryptophan fluorescence as probes in kinetic analyses of DNA polymerase β, *Biochemistry 41*, 11226−11235.
26. Bose-Basu, B., DeRose, E. F., Kirby, T. W., Mueller, G. A., Beard, W. A., Wilson, S. H., and London, R. E. (2004) Dynamic characterization of a DNA repair enzyme: NMR studies of [methyl-C-13]methionine-labeled DNA polymerase β, *Biochemistry 43*, 8911−8922.
27. Kim, S. J., Beard, W. A., Harvey, J., Shock, D. D., Knutson, J. R., and Wilson, S. H. (2003) Rapid segmental and subdomain motions of DNA polymerase beta, *J. Biol. Chem. 278*, 5072−5081.
28. Joyce, C. M., and Benkovic, S. J. (2004) DNA polymerase fidelity: Kinetics, structure, and checkpoints, *Biochemistry 43*, 14317−14324.
29. Showalter, A. K., and Tsai, M. D. (2002) A reexamination of the nucleotide incorporation fidelity of DNA polymerases, *Biochemistry 41*, 10571−10576.
30. Polesky, A. H., Dahlberg, M. E., Benkovic, S. J., Grindley, N. D. F., and Joyce, C. M. (1992) Side Chains Involved in Catalysis of the Polymerase Reaction of DNA Polymerase I from Escherichia coli, *J. Biol. Chem. 267*, 8417−8428.
31. Liu, J., and Tsai, M. D. (2001) DNA polymerase beta: Pre-steady-state kinetic analyses of dATPaS stereoselectivity and alteration of the stereoselectivity by various metal ions and by site-directed mutagenesis, *Biochemistry 40*, 9014−9022.
32. Hollfelder, F., and Herschlag, D. (1995) The nature of the transition state for enzyme-catalyzed phosphoryl transfer. Hydrolysis of *O*-aryl phosphorothioates by alkaline phosphatase, *Biochemistry 34*, 12255−12264.
33. Beard, W. A., and Wilson, S. H. (1995) Purification and domain-mapping of mammalian DNA polymerase beta, *Methods Enzymol. 262*, 98−107.
34. Upton, T. G., Osuna, J., Kashemirov, B. A., and McKenna, C. E. (2007) Synthesis of a series of methylene bisphosphonic acids and determination of stability constants by potentiometric titration. (In preparation).
35. Braun-Sand, S., Olsson, M. H. M., and Warshel, A. (2005) Computer modeling of enzyme catalysis and its relationship to concepts in physical organic chemistry, *Adv. Phys. Org. Chem. 40*, 201−245.
36. Warshel, A., Hwang, J. K., and Aqvist, J. (1992) Computer simulations of enzymatic reactions: Examination of linear free energy relationships and quantum mechanical corrections in the initial proton-transfer step of carbonic anhydrase, *Faraday Discuss. 93*, 225−238.
37. Albery, W. J. (1980) The application of the Marcus relation to reactions in solution, *Annu. Rev. Phys. Chem. 31*, 227−263.
38. Claessens, R. A. M. J., and Vanderlinden, J. G. M. (1984) Stability-constants of tin(II) and calcium diphosphonate complexes, *J. Inorg. Biol. 21*, 73−82.
39. Xiang, Y., Oelschlaeger, P., Florián, J., Goodman, M. F., and Warshel, A. (2006) Simulating the Effect of DNA Polymerase Mutations on Transition State Energetics and Fidelity: Evaluating Amino Acid Group Contribution and Allosteric Coupling for Ionized Residues in Human Pol β, *Biochemistry 45*, 7036−7048.
40. Florián, J., Goodman, M. F., and Warshel, A. (2002) Theoretical investigation of the binding free energies and key substrate-recognition components of the replication fidelity of human DNA polymerase β, *J. Phys. Chem. B 106*, 5739−5753.
41. Coxon, F. P., Thompson, K., and Rogers, M. J. (2006) Recent advances in understanding the mechanism of action of bisphosphonates, *Curr. Opin. Pharmacol. 6*, 307−312.
42. Fleisch, H. (2002) Development of bisphosphonates, *Breast Cancer Res. 4*, 30−34.
43. Castro, C., Smidansky, E., Maksimchuk, K. R., Arnold, J. J., Korneeva, V. S., Gotte, M., Konigsberg, W., and Cameron, C. E. (2007) Two proton transfers in the transition state for nucleotidyl transfer catalyzed by RNA- and DNA-dependent RNA and DNA polymerases, *Proc. Natl. Acad. Sci. U.S.A. 104*, 4267−4272.
44. Cleland, W. W. (1977) Determining the chemical mechanisms of enzyme-catalyzed reactions by kinetic studies, *Adv. Enzymol. Relat. Areas Mol. Biol. 45*, 273−387.
45. Hwang, J. K., and Warshel, A. (1996) How important are quantum mechanical nuclear motions in enzyme catalysis, *J. Am. Chem. Soc. 118*, 11745−11751.
46. Klahn, M., Rosta, E., and Warshel, A. (2006) On the mechanism of hydrolysis of phosphate monoesters dianions in solutions and proteins, *J. Am. Chem. Soc. 128*, 15310−15323.
47. Aqvist, J., Kolmodin, K., Florián, J., and Warshel, A. (1999) Mechanistic alternatives in phosphate monoester hydrolysis: What conclusions can be drawn from available experimental data, *Chem. Biol. 6*, R71−R80.
48. Kraynov, V. S., Showalter, A. K., Liu, J., Zhong, X. J., and Tsai, M. D. (2000) DNA polymerase β: Contributions of template-positioning and dNTP triphosphate-binding residues to catalysis and fidelity, *Biochemistry 39*, 16008−16015.
49. Beard, W. A., Shock, D. D., Vande Berg, B. J., and Wilson, S. H. (2002) Efficiency of correct nucleotide insertion governs DNA polymerase fidelity, *J. Biol. Chem. 277*, 47393−47398.
50. Mihai, C., Kravchuk, A. V., Tsai, M. D., and Bruzik, K. S. (2003) Application of Bronsted-type LFER in the study of the phospholipase C mechanism, *J. Am. Chem. Soc. 125*, 3236−3242.
51. Daniele, P. G., Rigano, C., and Sammartano, S. (1985) Ionic-strength dependence of formation-constants - Alkali-metal complexes of ethylenediaminetetraacetate, nitrolotriacetate, diphosphate, and tripolyphosphate in aqueous-solution, *Anal. Chem. 57*, 2956−2960.

BI7014162